Water bilayer structures

H-down, H-up and half-dissociated water bilayer structures

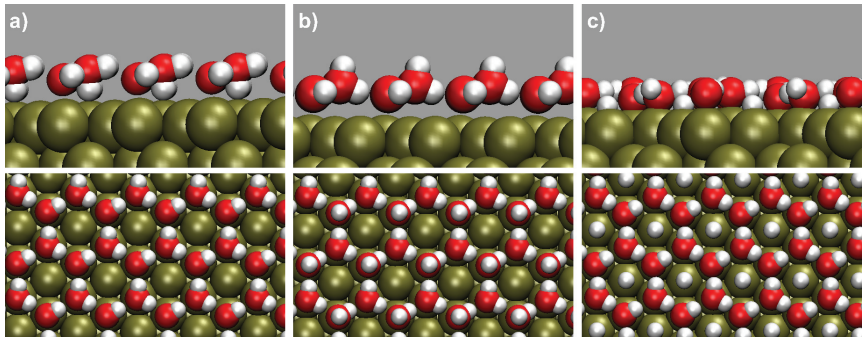

H-down and H-up layer often energetically almost degenerate

PBE vs. RPBE with and without dispersion corrections

Katrin Tonigold and Axel Groß, ,J. Comput. Chem. **33**, 695-701 (2012) .

Role of dispersion effects in the water-water and the water-metal interaction

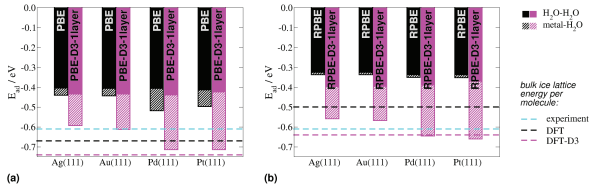

Comparison with ab initio calculations for dimers

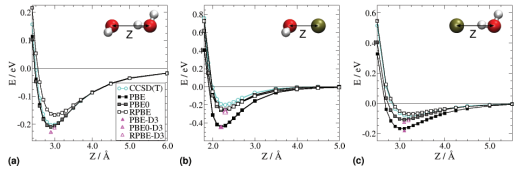

RPBE-D3 exhibits acceptable properties

Pt(111) covered by water bilayers

Yoshihiro Gohda, Sebastian Schnur, Axel Groß, Faraday Diss. **140**, 233 (2009).

Geometric structure

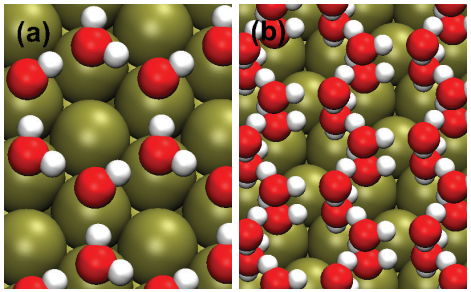

Structure of a water bilayer and double bilayer on Pt(111)

Electronic structure

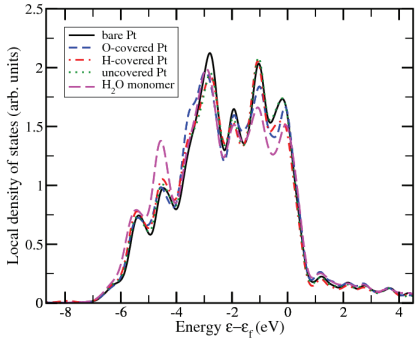

Pt(111) local d-band density of states

Electronic structure of Pt(111) hardly changed by the adsorption of water

Water-induced work function change

H-down water bilayer

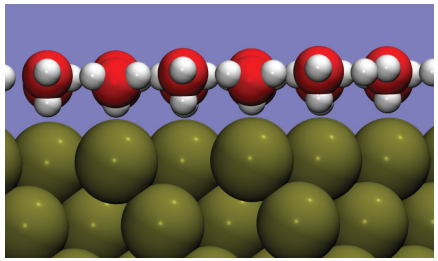

$E_{ads}^{H_2O}$ = -487 meV

$\Delta\Phi$ = -0.23 eV

H-up water bilayer

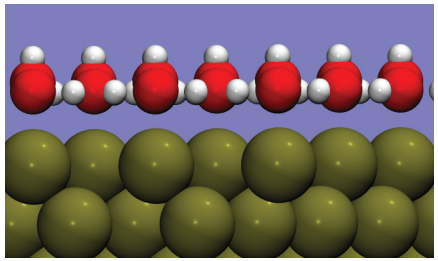

$E_{ads}^{H_2O}$ = -450 meV

$\Delta\Phi$ = -2.27 eV

2 eV difference in work function change between H-down and H-up bilayers, but both bilayers lead to a reduction in the work function of Pt(111), although dipole moments of the two free bilayers have opposite signs

Water-induced charge density difference plots

$$\Delta\rho = \rho(\mathrm{H_2O/Pt(111)}) - (\rho(\mathrm{H_2O}) + \rho(\mathrm{Pt(111)}))$$

H-down water bilayer

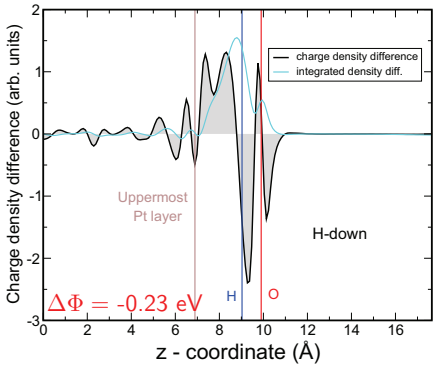

H-up water bilayer

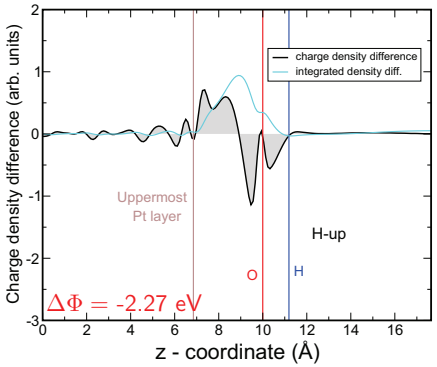

Charge accumulation between water bilayer and Pt(111)

Water orientation as a function of the electric field

A. Roudgar and A. Groß, Chem. Phys. Lett. **409**, 157 (2005)

Total energy of the H-down and H-up water bilayers as a function of an external electric field

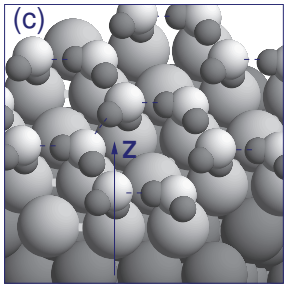

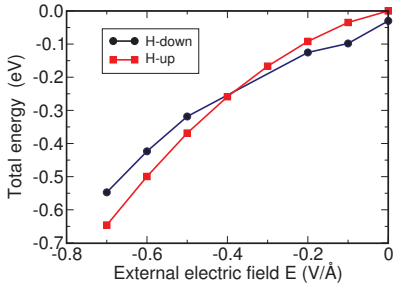

Field-induced water reorientation confirmed by experiment for H_2O/Ag(111)

K. Morgenstern and J. Nieminen, J. Chem. Phys. **120**, 10786 (2004)

Proposal: Charge control of the water monolayer/Pd interface

J.S. Filhol and M.-L. Bocquet, Chem. Phys. Lett. **438**, 203 (2007)

Chemical trends in water-induced work function change

Sebastian Schnur and Axel Groß, New J. Phys **11**, 125003 (2009).

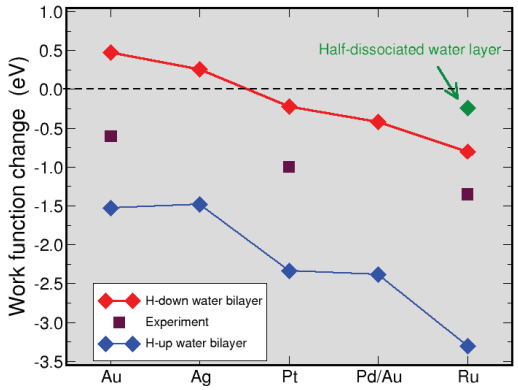

Overall work function change correlates with water-metal interaction strength, but surprisingly large discrepancies to experimental results

Ab initio molecular dynamics simulations (AIMD) of water on Ag(111)

T = 1.5 ps

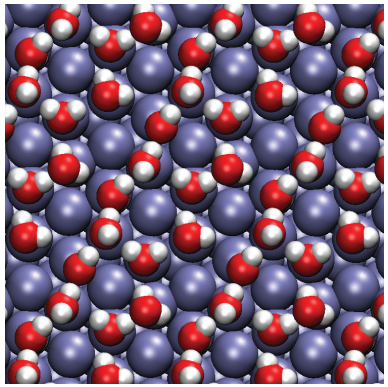

T = 7.5 ps

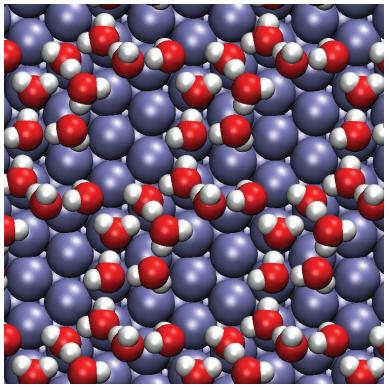

Hexagonal ice-like structure at room temperature broken up after 7.5 ps

AIMD simulations of water on Pt(111)

T = 1.5 ps

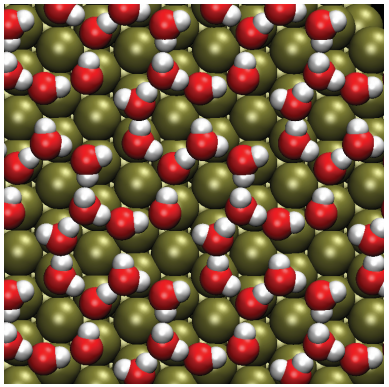

T = 7.5 ps

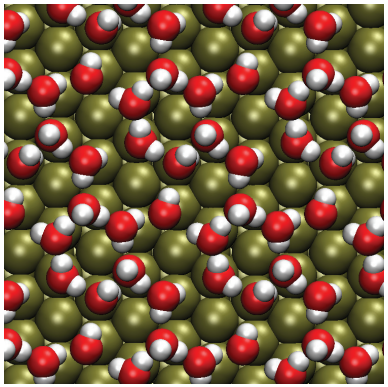

Hexagonal ice-like structure at room temperature still intact after 7.5 ps

AIMD simulations of water layers at room temperature

Sebastian Schnur and Axel Groß, New J. Phys **11**, 125003 (2009).

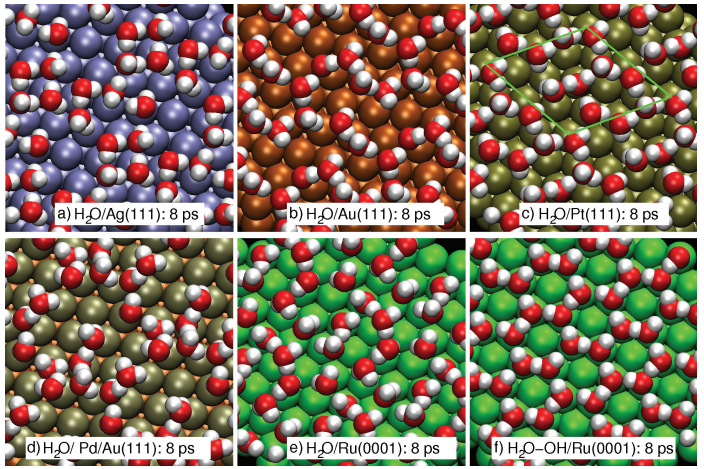

On noble metal surfaces (Au, Ag), ice-like bilayer structure not stable at room temperature.

Water trajectories at room temperature

Sebastian Schnur and Axel Groß, New J. Phys **11**, 125003 (2009).

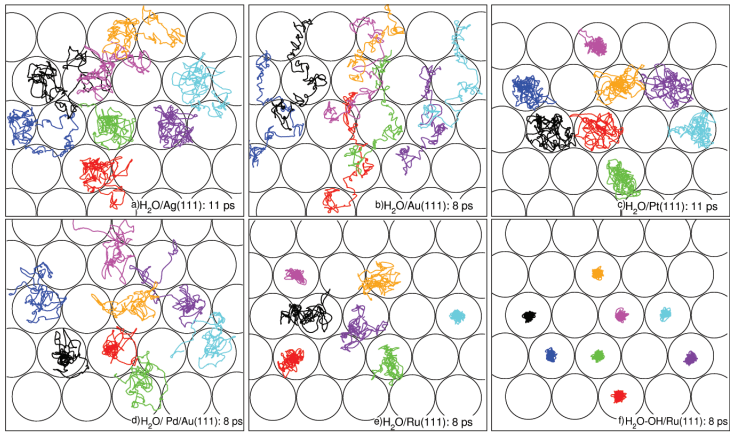

On noble metal surfaces (Au, Ag), ice-like bilayer structure not stable at room temperature.

Vibrational spectra of water bilayers on (111) substrates

Sebastian Schnur and Axel Groß, New J. Phys **11**, 125003 (2009).

Spectra based on AIMD runs of approximately 10 ps in a $2\sqrt{3} \times 2\sqrt{3}R30°$ unit cell

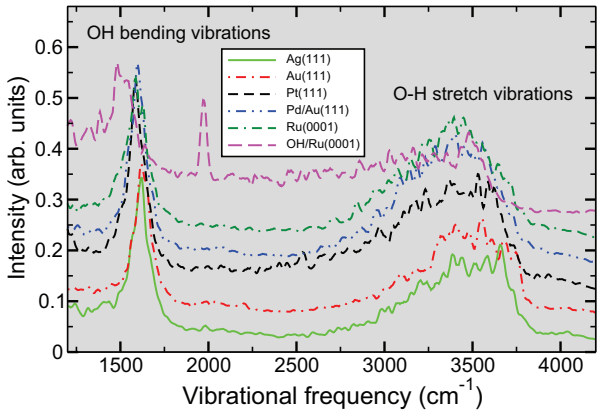

Stronger red-shift for Pt, Pd/Au and Ru than for noble metals Au and Ag

Time evolution of work function change

Sebastian Schnur and Axel Groß, New J. Phys **11**, 125003 (2009).

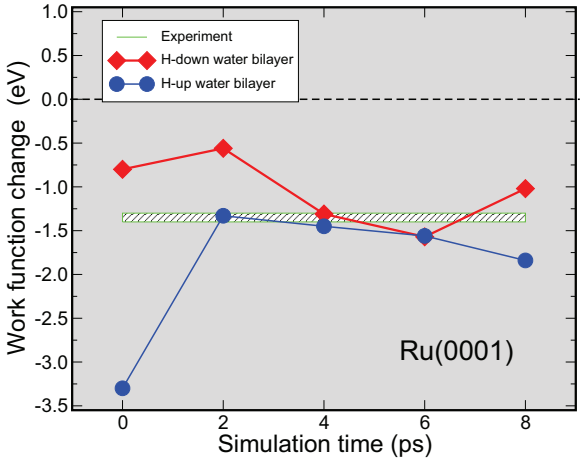

Thermal averaging ⇒ good agreement between theory and experiment

Exp.: W. Hoffmann and C. Benndorf, Surf. Sci. **377-379**, 681 (1997); Y. Lilach *et al.*, J. Phys. Chem. B **105**, 2736 (2001).

Work function change for thermalized water layers

Sebastian Schnur and Axel Groß, Catal. Today **165**, 129-137 (2011).

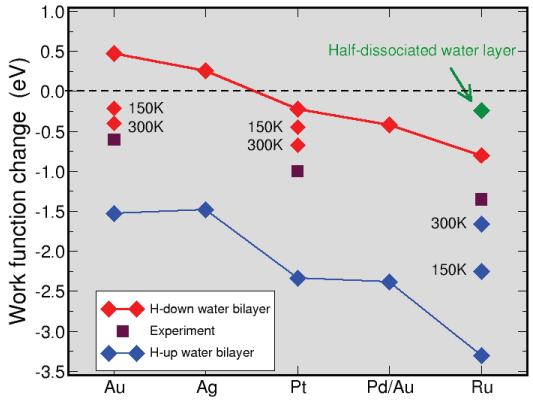

Averaging done over 2 ps ab initio molecular dynamics runs

Water on other metal substrates: H_2O/Pb

Xiaohang Lin and Axel Groß, in preparation

H_2O/Pb(111)

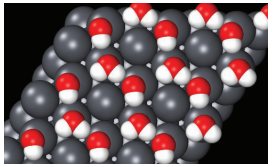

$\Theta_{H_2O} = 2/3$

$E_{ads} = -0.254\,\text{eV}$

H_2O/Pb(100)

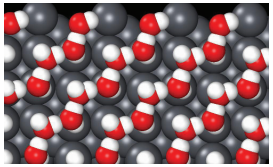

$\Theta_{H_2O} = 1$

$E_{ads} = -0.359\,\text{eV}$

H_2O/Pb(100)

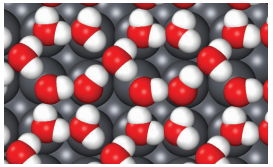

$\Theta_{H_2O} = 5/4$

$E_{ads} = -0.396\,\text{eV}$

Nearest-neighbor distance in Pb ($d_{NN} = 3.50\,\text{Å}$) much larger than for late transition metals

⇒ Nominally higher water coverages per substrate atom stable

Water on other metal substrates: H_2O/Au(100)

Xiaohang Lin and Axel Groß, Surf. Sci. **606**, 886-891 (2012).

$T = 0\,\text{K}$ $T = 140\,\text{K}$ $T = 300\,\text{K}$

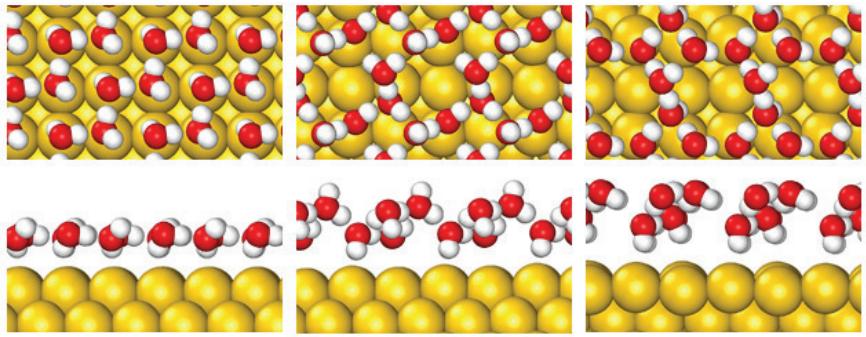

No hexagonal water arrangement on Au(100), 2×2 unit cell most probably insufficient

Water on other metal substrates: H_2O/Au(511)

Xiaohang Lin and Axel Groß, Surf. Sci. **606**, 886-891 (2012).

$T = 0\,\mathrm{K}$ $T = 140\,\mathrm{K}$ $T = 300\,\mathrm{K}$

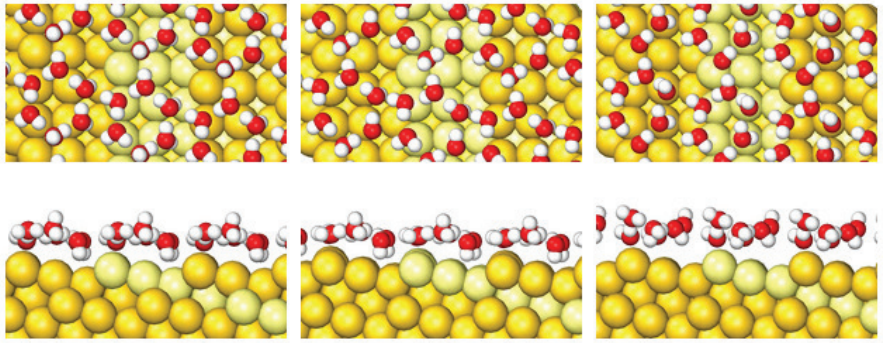

Stable water structure on Au(511), consisting of hexagons, rectangles and octagons

Vibrational spectra of water on Au(100) and Au(511)

Vibrational spectra derived from AIMD runs at $T = 140\,\mathrm{K}$

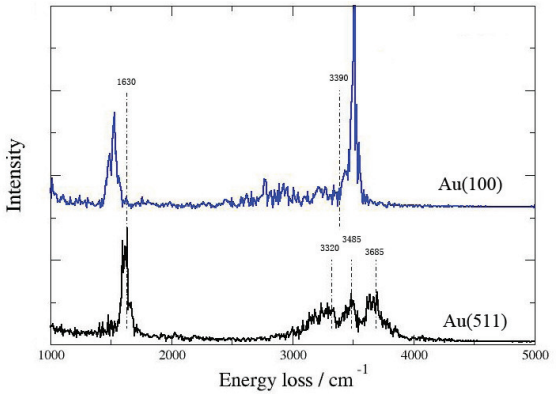

Dashed lines: experimentally observed peaks (H. Ibach, Surf. Sci. **604**, 377 (2010).)

Mode-splitting in O-H stretch region around $3500\,\mathrm{cm}^{-1}$ on Au(511) reflects coexistence of hydrogen-bonded and non-hydrogen bonded H atoms in water layer

H adsorption in the presence of a water overlayer

A. Roudgar and A. Groß, Surf. Sci. **597**, 42 (2005)

Water structures on Pd/Au(111)

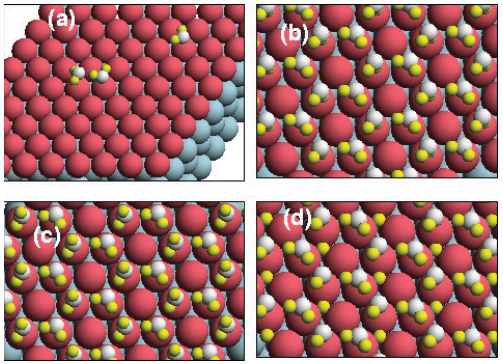

H_2O structure: a) monomer and dimer, b) H-down bilayer (ice Ih), c) H-up bilayer, d) half-dissociated bilayer

H adsorption energies

θ_{H_2O}	$E_{ads}^{H_2O}$	$E_{ads}^{H\,fcc}$	$E_{ads}^{H\,hcp}$
1/4	-0.308	-0.634	-0.592
1/3	-0.295	-0.606	-0.610
1/2	-0.419	-0.582	-0.602
1	+3.135	–	–
3/4	-0.465	-0.561	–
2/3(b)	**-0.528**	**-0.633**	**-0.596**
2/3(c)	-0.499	–	–
2/3(d)	-0.327	–	–
0	–	**-0.690**	**-0.655**

H_2O adsorption energies in eV/H_2O and H adsorption energies ($\theta_H = 1/3$) in eV/atom on Pd/Au(111)

H adsorption energies only slightly changed by the presence of water

CO adsorption in the presence of a water overlayer

A. Roudgar and A. Groß, Chem. Phys. Lett. **409**, 157 (2005)

CO/water structures on Pd/Au(111)

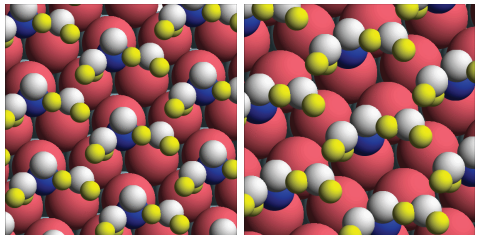

CO/H_2O structures (H-down): a) CO in fcc hollow, b) CO on-top

CO adsorption energies

site	E_{ads}^{CO} H-down	E_{ads}^{CO} H-up	E_{ads}^{CO} clean
fcc	-1.831	-1.894	-2.023
hcp	-1.866	-1.923	-2.043
bridge	—	—	-1.827
on-top	-1.243	—	-1.413

CO adsorption energies ($\theta_{CO} = 1/3$) in eV/molecule on H_2O/Pd/Au(111)

Both H_2O and CO are polar molecules. Still the dipole-dipole interaction between CO and H_2O in the ice-Ih structure on Pd/Au(111) only $\lesssim 50$ meV

Water relaxation upon CO and H adsorption

A. Roudgar and A. Groß, Chem. Phys. Lett. **409**, 157 (2005)

CO/water and H/water structures on Pd/Au(111)

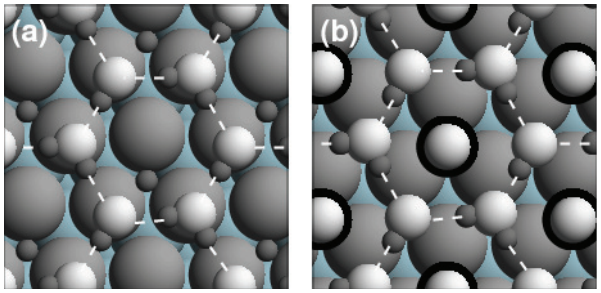

Relaxed water structures in the presence of CO and H

Because of the strong CO-metal interaction, a shifted water bilayer is energetically more favorable

Potential energy surface of H_2/Pt(111)

Yoshihiro Gohda, Sebastian Schnur, Axel Groß, Faraday Diss. **140**, 233 (2009).

Without water | One water bilayer | Two water bilayers

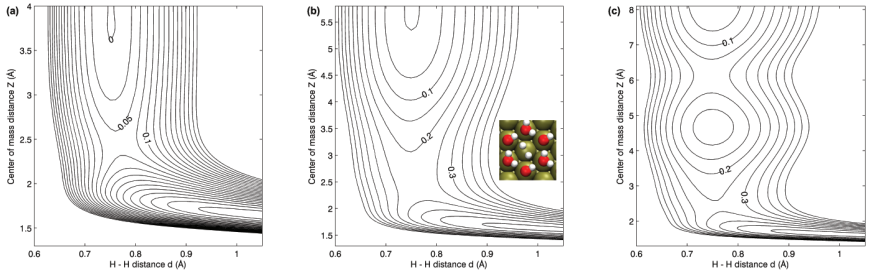

PES as a function of the H_2 distance from the surface and the H-H separation

Barrier height: Superposition of H_2/Pt(111) dissociation barrier and H_2-water repulsion

Disordered water structures

Disordered structures created by removing water molecules from the two water bilayers

Structure

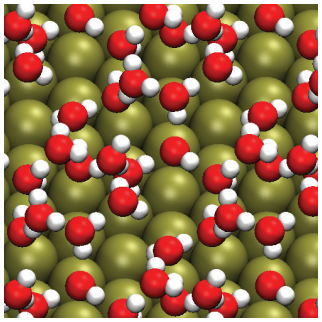

Example of a disordered water structure

H_2 dissociation barrier heights

Lower layer							
#	0	1	1	2	2	2	3
E_b	270	296	284	276	275	323	189
Upper layer							
#	0	0	1	1	2	3	3
E_b	173	172	162	139	97	9	0

Dependence of the dissociation barriers E_b in meV in the lower and the upper water layer on the number of molecules removed from the water layers (#).

Barrier heights significantly lowered for disordered water structures ⇒ thermal averaging required to determine free energy barriers

H_2 dissociation at further water/metal interfaces

H_2/Ru(0001) | H_2/Pd/Au(111)

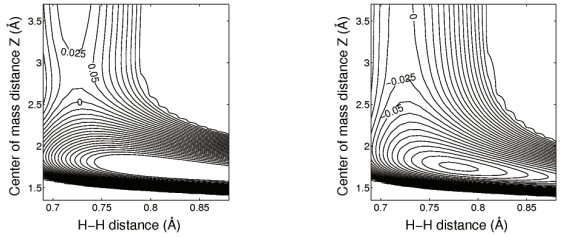

H_2/H_2O/Ru(0001) | H_2/H_2O/Pd/Au(111)

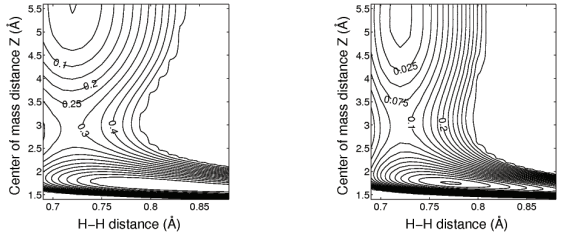

Barriers for H_2 dissociation at water/metal interfaces

		ΔE (meV)	z (Å)	Metal NN distance (Å)
Pt(111)	clean	54	2.4	2.77
Pt(111)	H-down	221	2.5	
Ru(0001)	clean	30	2.8	
Ru(0001)	H-down	290	3.0	2.68
Ru(0001)	H-up	369	2.8	
Pd/Au(111)	clean	0	-	2.86
Pd/Au(111)	H-down	91	3.0	

Strong correlation between metal lattice constant (≡ size of the water ring) and the change of the H_2 dissociation barrier when a water layer is included

H_2 dissociation barrier at water/metal interfaces at room temperature

Sebastian Schnur and Axel Groß, Catal. Today, **165**, 129 (2011).

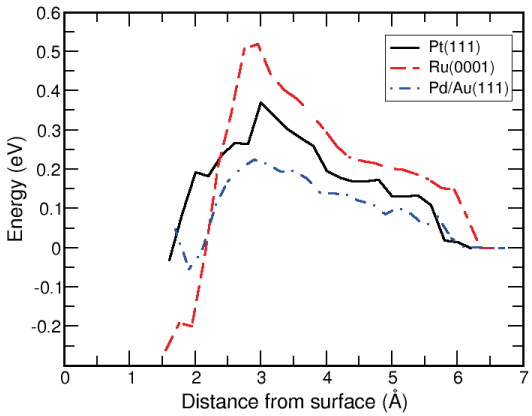

Free energy determined by constrained AIMD runs along dissociation path

Further increase of barriers by 150 meV due to thermal motion of the water atoms

Ab initio molecular dynamics simulations of H_2 dissociation on water-covered Pt(111)

Trajectory

Discussion

H_2 dissociation through thermalized disordered water layer

After dissociation, H atoms can move almost freely beneath the water layer

H atoms end up at top sites

Disordered water layer rearranges upon H adsorption

Varying electrode potentials

Electrochemistry: electrode potential additional important external parameter

Varying electrode potentials

Electrochemistry: electrode potential additional important external parameter

Theoretical consideration of electrode potential not trivial

Varying electrode potentials

Electrochemistry: electrode potential additional important external parameter

Theoretical consideration of electrode potential not trivial

Effective incorporation of electron potential is possible

Varying electrode potentials

Electrochemistry: electrode potential additional important external parameter

Theoretical consideration of electrode potential not trivial

Effective incorporation of electron potential is possible

Differential adsorption energies H/Pt(111)

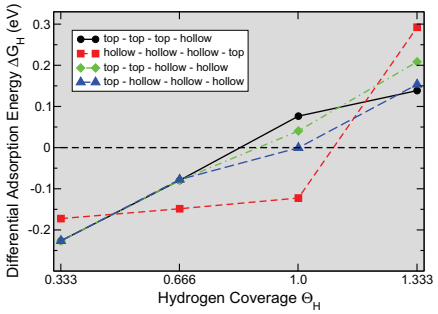

At standard conditions, hydrogen evolution

$$\mathrm{H}^+ + e^- \leftrightarrow \frac{1}{2}\mathrm{H}_2$$

is in equilibrium

$\Rightarrow$ processes with $\Delta G_\mathrm{H} < \mu_\mathrm{H} = -eU$ occur under equilibrium conditions

Change in electron number n between reactants and product considered via $\Delta G = \Delta G(0) + neU$

At standard conditions, a Pt(111) electrode is covered by a hydrogen layer

Chemical trends in the hydrogen evolution

J.K. Nørskov *et al.*, J. Electrochem. Soc. **152**, J23 (2005).

Free energy diagram for hydrogen evolution at equilibrium (U=0 vs NHE)

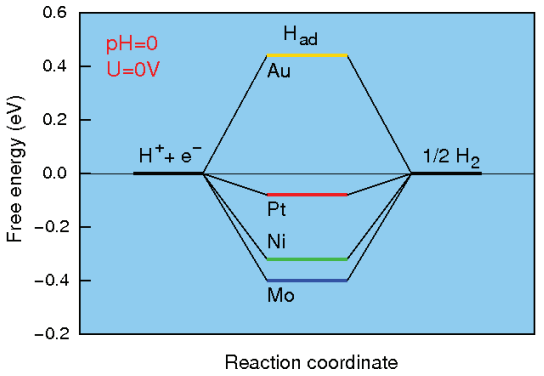

On Pt(111), hydrogen evolution in equilibrium with the intermediate H adsorption state

$\Rightarrow$ Exceptional role of Pt as an electrocatalyst

Charged systems in periodic DFT calculations

A.Y. Lozovoi *et al.*, J. Chem. Phys. **115**, 1661 (2001)

Charging up the slabs also leads effectively to a variation in the electrode potential, but in periodic calculations the unit cell has to be neutral

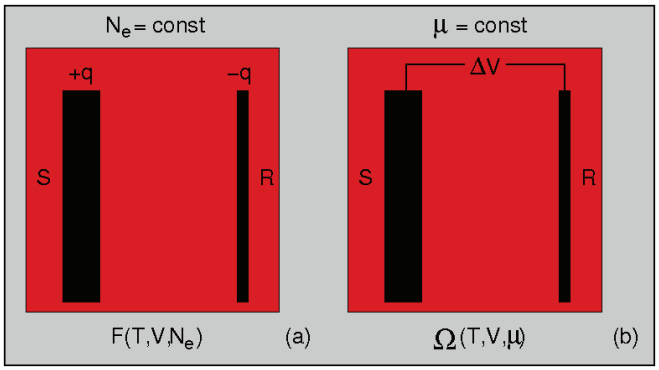

Two different modes are possible to treat charged slabs corresponding to a canonical and a grand-canonical formulation

Reconstruction of charged surfaces: Pt(110) and Au(110)

A.Y. Lozovoi and A. Alavi, Phys.Rev. B **68**, 245416, (2003)

Setup of supercell calculations

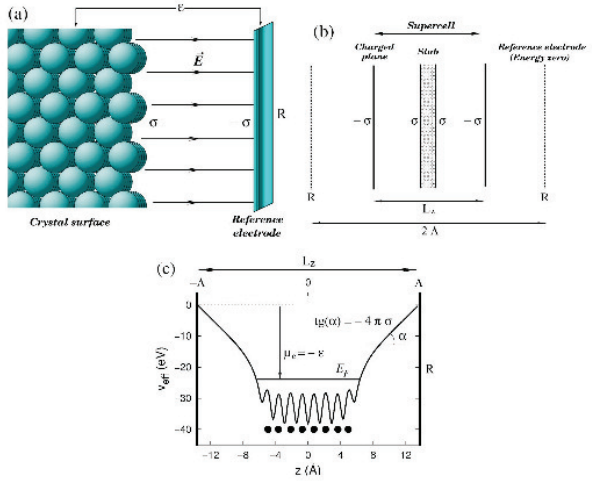

Au(110): Lifting of (1×2) missing-row reconstruction

A.Y. Lozovoi and A. Alavi, Phys.Rev. B **68**, 245416, (2003)

Constant charge

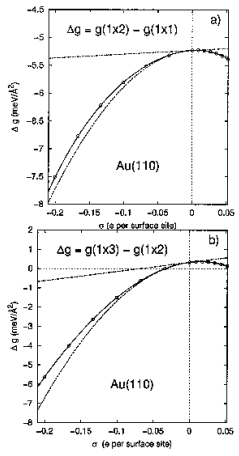

Constant potential

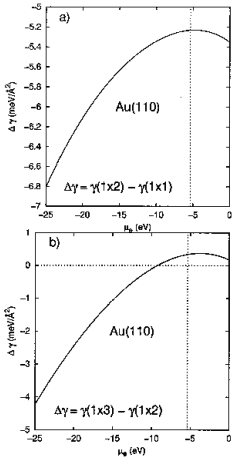

Analogous bevavior in constant-charge and constant-potential mode

Interface with a constant charge background

C.D. Taylor *et al.*, Phys. Rev. B **73**, 165402 (2006).

Potential with and without a water layer

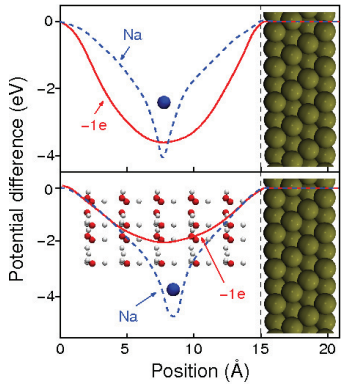

Constant charge background: automatic default procedure in periodic DFT codes to compensate a charged system

Poisson equation for region with a constant charge background:

$$\nabla^2\phi(\mathbf{x}) \;=\; 4\pi\rho_o\,. \qquad (1)$$

General solution:

$$\phi(\mathbf{x}) \;=\; 4\pi\rho_o\Big(\sum_{i,j} C_{i,j}x_ix_j + \sum_i C_ix_i + C_0\Big)\,. \quad (2)$$

Artefacts due to parabolic solution outside the metal electrodes reduced through the presence of polarizable water layers

Energy expression in the presence of a constant charge background

C.D. Taylor *et al.*, Phys. Rev. B **73**, 165402 (2006).

$$\frac{\partial E_{\rm DFT}}{\partial q} = \frac{\partial E_{\rm slab}}{\partial q} + \frac{\partial E_{\rm slab-bg}}{\partial q} + \frac{\partial E_{\rm bg}}{\partial q} , \quad (3)$$

$E_{\rm slab}$: energy of the charged water/electrode system, $E_{\rm slab-bg}$: interaction between the system and the background charge, and $E_{\rm bg}$ energy of the background.

$$E_{\rm slab-bg} = \int \rho_{\rm bg} V_{\rm slab} d^3x , \quad E_{\rm bg} = \int \rho_{\rm bg} V_{\rm bg} d^3x , \quad (4)$$

$V_{\rm slab}$: electrostatic potential of the charged water/electrode system in the absence of the background charge. Note that $\rho_e = -\rho_{\rm bg} = q$.

$$\Rightarrow \frac{\partial E_{\rm DFT}}{\partial q} = \mu - \int \frac{V_{\rm tot}}{\Omega} d^3x . \quad (5)$$

$$\Rightarrow \text{Grand canonical free energy } E = \int_0^q \mu dQ = E_{\rm DFT} + \int_0^q \left[\int \frac{V_{\rm tot}}{\Omega} d^3x \right] dQ . \quad (6)$$

Electrode potential for a constant background charge

C.D. Taylor *et al.*, Phys. Rev. B **73**, 165402 (2006).

"Double-reference method"

Electrostatic potential profile

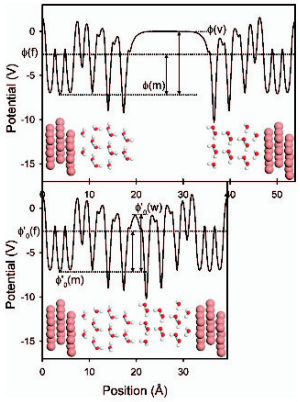

First reference: vacuum level for uncharged system

$$\phi_0(m) = \phi(m) = \phi'(m) - \phi'(v) \quad (7)$$

Index 0: system without vacuum

$$\phi_0(z) = \phi'_0(z) - \phi'_0(m) + \phi_0(m)$$
$$= \phi'_0(z) - \phi'_0(m) + \phi'(m) - \phi'(v) \quad (8)$$

Second reference: Fixed region far from the electrode at its position in the $q = 0$ calculation (potential $\phi_0(w)$) while the rest of the system is relaxed in response to the applied charge

$$\phi_q(z) = \phi'_q(z) - \phi'_a(w) + \phi_0(w) \quad (9)$$

Absolute potential:

$$\phi_{\rm NHE} = -4.85{\rm eV} - \phi_q \quad (10)$$

Applications: Electrochemical Activation of Water over Pd

J.S. Filhol and M. Neurock, Angew. Chem. Int. Ed. **402**, 402 (2006)

Evolution of the structure of the palladium/hydroxide interface as a function of applied potential

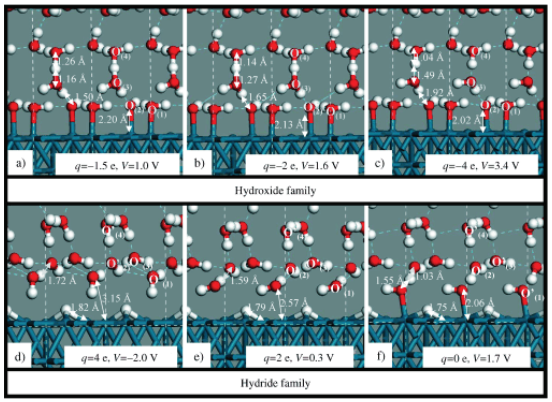

H_2O/Pd/Au structure and H_2O-Pd/Au distance as a function of an external electric field

Oxygen dissociation at an electrode surface

S.A. Wasileski and M.J. Janik, PCCP **10**, 3613 (2008).

O_2 dissociation on Pt(111) in the presence of water and Na at various potentials

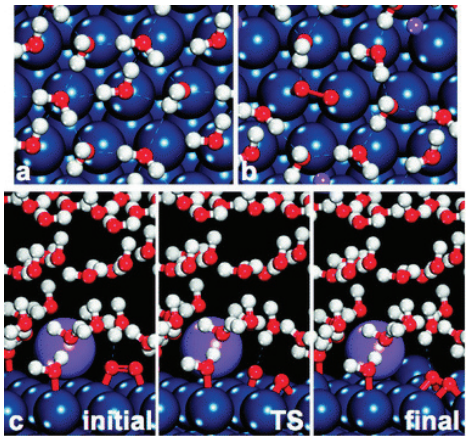

O_2 dissociation path with coadsorbed Na

Potential dependence of O_2 dissociation

S.A. Wasileski and M.J. Janik, PCCP **10**, 3613 (2008).

Potential dependence of initial, transition and final state energies for O_2 dissociation on solvated Pt(111)

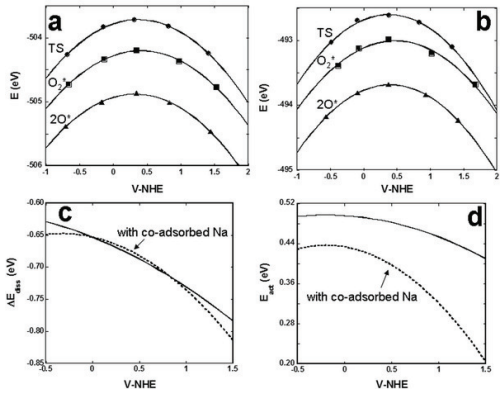

Variation in the structure along a reaction path can lead to changes in the workfunction corresponding to a variation in the electrode potential

Quadratic fit referenced vs. NHE

$$E(\phi) = A\phi^2 + B\phi + C \qquad (11)$$

in order to generate continuous energy vs. potential curve

Oxygen dissociation activation energy

S.A. Wasileski and M.J. Janik, PCCP **10**, 3613 (2008).

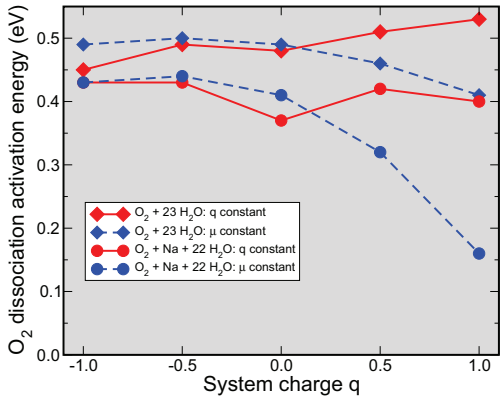

Reduction of the O_2 dissociation barrier in the presence of Na

Significant difference between results for constant charge and constant chemical potential at the potential of the initial state

Explicit consideration of counter ions

E. Skúlason, J. Rossmeisl, J.K. Nørskov *et al.*, PCCP **9**, 3241 (2007); CPL **466**, 68 (2008)

Change of electrode potential by varying the number of protons/electrons in the double layer

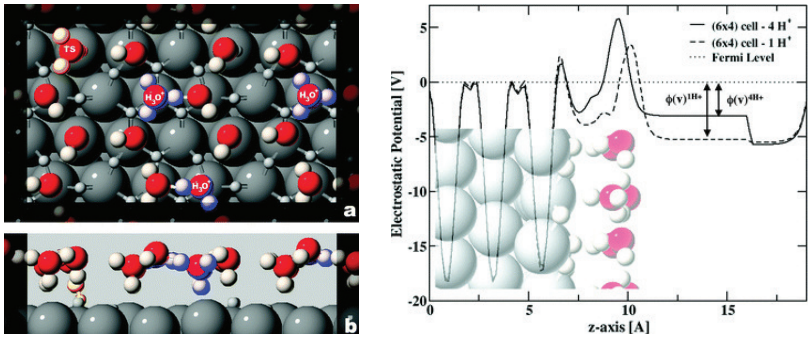

Excess H atoms are included in the water layer which results in the formation of solvated protons in the water layer and transfer of electrons to the metal

Problem: only one water bilayer, protons confined to the first water bilayer, electrode potential can vary along reaction paths

Tafel reaction as a function of the electrode potential

E. Skúlason, J. Rossmeisl, J.K. Nørskov *et al.*, PCCP **9**, 3241 (2007).

Tafel mechanism: $2H_{ad} \rightarrow H_2$

Reaction path

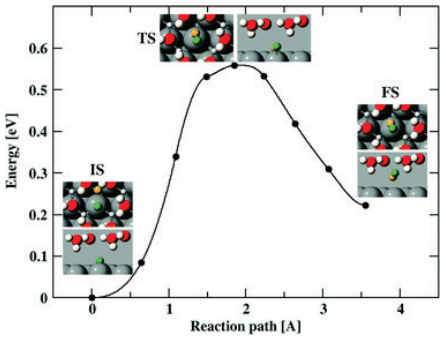

Activation energy

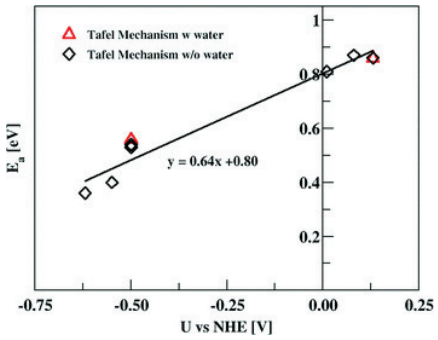

Linear dependence of activation energy on electrode potential

Non-periodic slab calculations with effective screening medium

O.Sugino *et al.*, Surf. Sci. **601**, 5237 (2007); PCCP **10**, 3609 (2008).

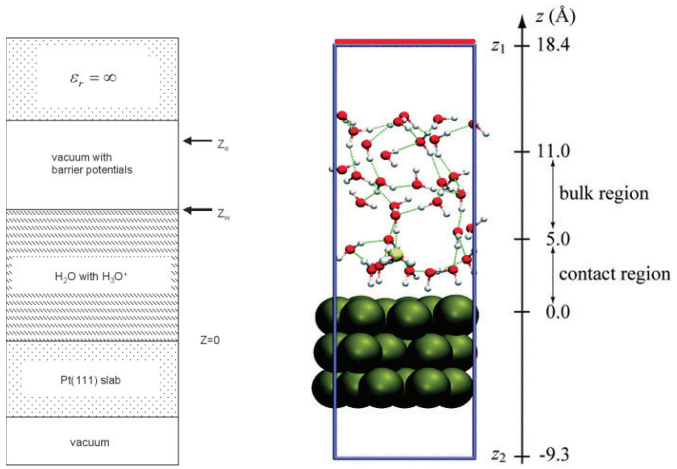

Structure of the water/platinum interface

M. Otani, O.Sugino *et al.*, PCCP **10**, 3609 (2008).

AIMD snapshot

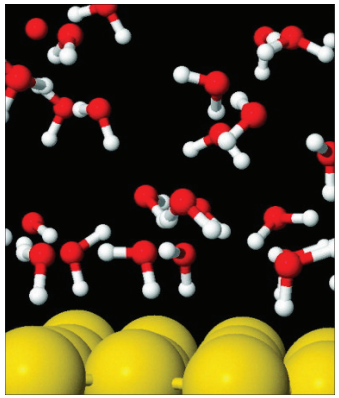

Structure: distribution function

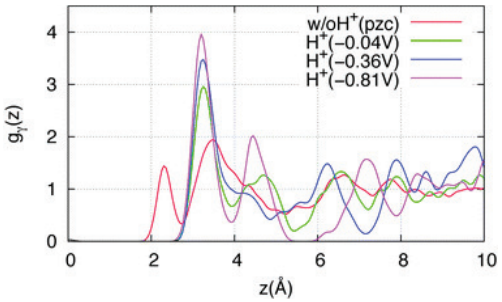

No bias: O-down structure stable

Negative bias: H-down structure stable, moderate increase of the density of contact layer with increasing bias

Boundary-matching scattering density functional method

Y. Gohda and S. Watanabe, PRL **85**, 1750 (2000); J. Phys.: Condens. Matter **16**, 4685 (2004)

BSDF method: Scattering solution of Kohn-Sham states with external electric field imposed as a real-space boundary condition

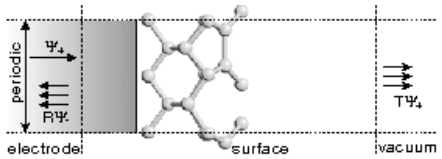

Application: Metal-induced gap states (MIGS) at the Si-Al interface

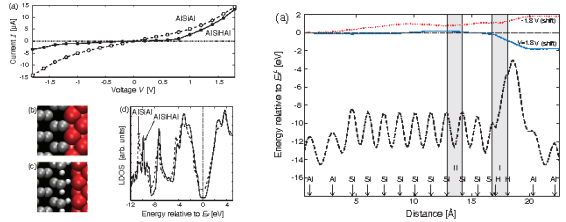

Y. Gohda, S. Watanabe and A. Groß, PRL **101**, 166801 (2008).

Charge-induced effects

Sebastian Schnur and Axel Groß, New J. Phys **11**, 125003 (2009).

Countercharge modeled by uniform charge background

O-wall distribution function

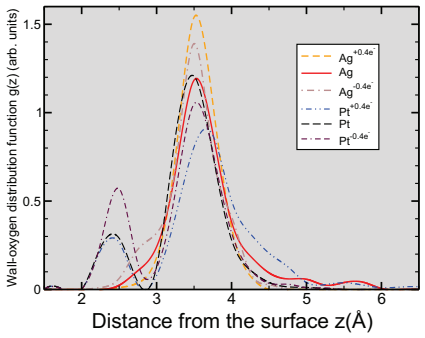

Vibrational spectra

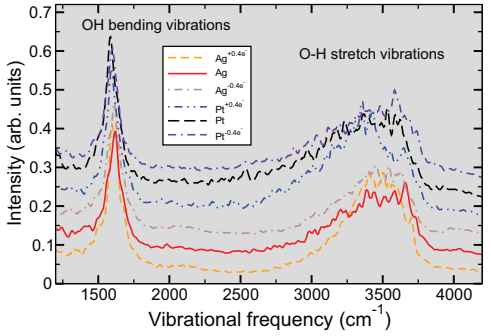

Problem: artefacts due to uniform charge background

Implementation: Explicit counter charge in supercell

S. Schnur and A. Groß, Catal. Today, **165**, 129 (2011).

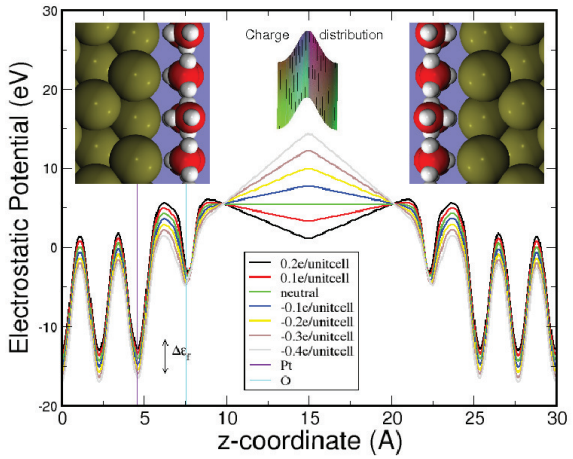

Advantage: Separation of counter electrode and considered system

Application: stability of water layers as a function of the electrode potential

S. Schnur and A. Groß, Catal. Today, **165**, 129 (2011).

$$E_{\text{free}} = E_{\text{total}} - \mu q$$

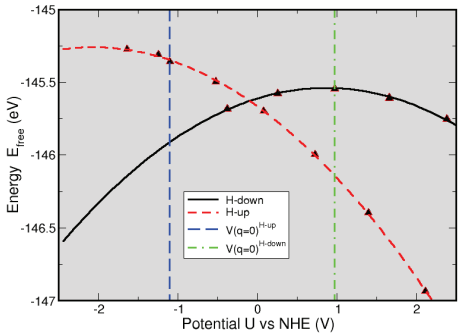

Capacities derived from these curves are a factor of two smaller than experimental results
Agreement improved when results from AIMD runs are used

Volmer reaction on Pt(111)

S. Schnur and A. Groß, Catal. Today, **165**, 129 (2011).

Hydrogen evolution according to the Volmer-Tafel-mechanism

$$\mathrm{H_3O^+} + e^- \leftrightarrow \mathrm{H_{ad}} + \mathrm{H_2O} \quad \text{Volmer reaction} \tag{12}$$

$$2\mathrm{H_{ad}} \leftrightarrow \mathrm{H_2} \quad \text{Tafel reaction} \tag{13}$$

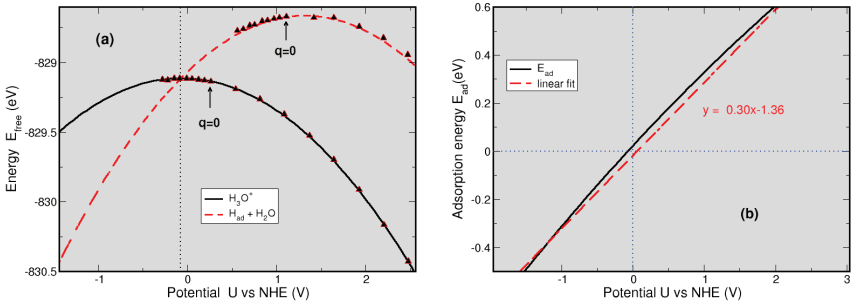

On Pt(111), hydrogen evolution in equilibrium with the intermediate H adsorption state
⇒ Exceptional role of Pt as an electrocatalyst

J.K. Nørskov *et al.*, J. Electrochem. Soc. **152**, J23 (2005).

Water structure on H-covered Pt(111)

T. Roman and A. Groß, Catal. Today **202**, 183190 (2013).

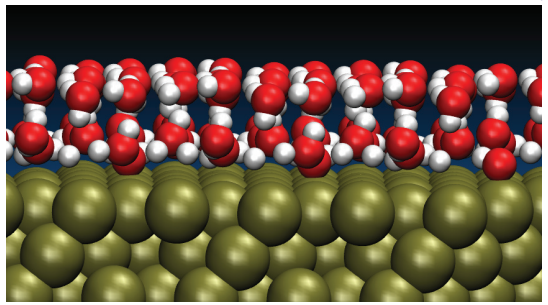

Water structure at 300 K on clean Pt(111)

Water structure on H-covered Pt(111)

T. Roman and A. Groß, Catal. Today **202**, 183190 (2013).

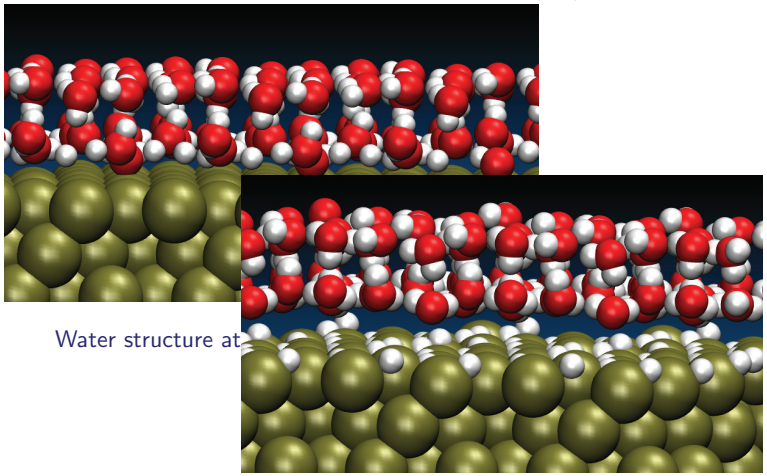

Water structure at

Water structure at 300 K on H-covered Pt(111)

Adsorption of anions at electrode-electrolyte interfaces

T. Roman, A. Groß, and P. Bagus, in preparation

Workfunction change

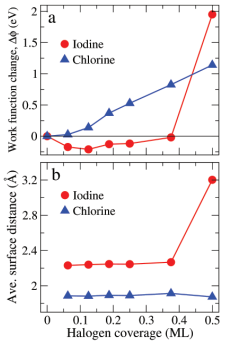

Laterally projected charge density difference

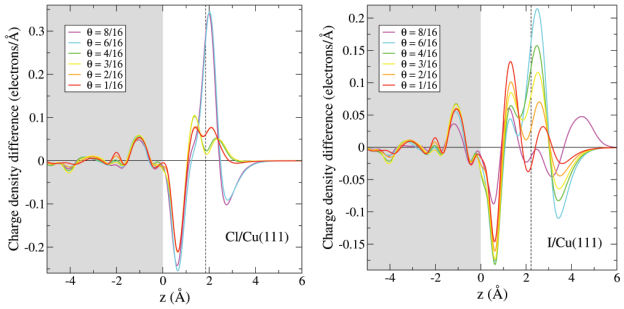

Iodine-induced work function change exhibits unexpected trend

ulm university universität ulm

Elementary reaction steps in electrocatalysis: Theory meets experiment

DFG Research Unit FOR 1376

Theory

Ulm University

Axel Groß

Timo Jacob

Elizabeth Santos

Wolfgang Schmickler

University Duisburg-Essen

Eckhard Spohr

Experiment

Ulm University

R. Jürgen Behm

Harry E. Hoster

Zenonas Jusys

Ludwig Kibler

Elizabeth Santos

Technical University of Munich

Ulrich Stimming

Helmholtz Institute Ulm (HIU)

HIU Electrochemical Energy Storage – established January 1, 2011

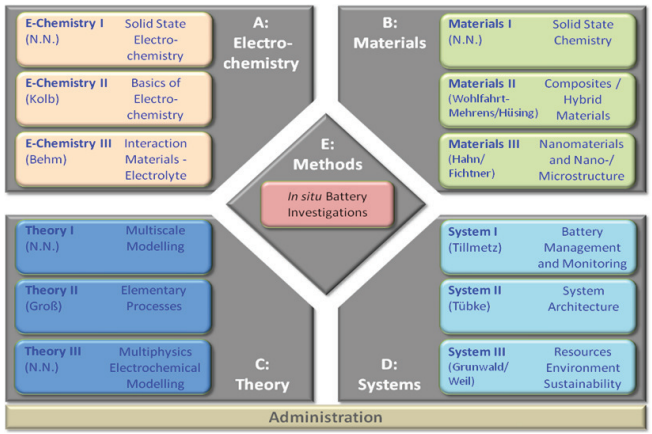

Project in the HIU: Structure of $LiMnPO_4$ nanocrystallites

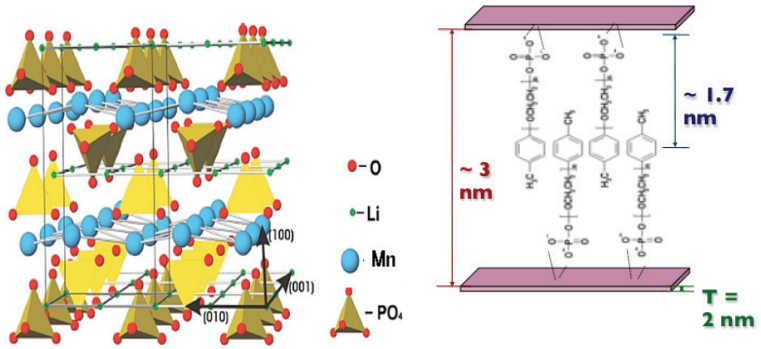

Preparation of nano-sized $LiMnPO_4$ crystallites in order to reduce transport limitation

Collaboration with N. Hüsing (Univ. of Salzburg) and M. Wohlfahrt-Mehrens (ZSW Ulm)

Stability of $LiMnPO_4$(010) surface terminations

$LiMnPO_4$(010) crystal cannot be cut into a slab with equivalent top and bottom termination

Top termination:	Bottom termination:
T1: -Li	B1: +Li-2$LiMnPO_4$
T2: -$LiMnPO_4$	B2: -$LiMnPO_4$
T3: -Li-$LiMnPO_4$	B3: +Li-$LiMnPO_4$

Surface free energies as a function of the environment

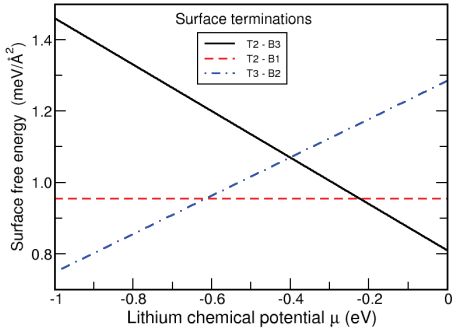

$LiMnPO_4$(010)

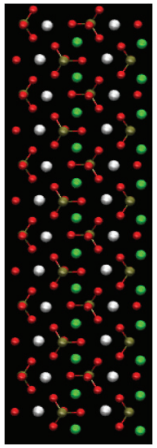

Self-assemblied monolayers (SAM)

H.-G. Boyen, P. Ziemann, U. Wiedwald, V. Ivanova, D. M. Kolb, S. Sakong, A. Groß, A. Romanyuk, M. Büttner, P. Oelhafen, Nature Materials **5**, 394 (2006).

Metal-SAM-metal junction

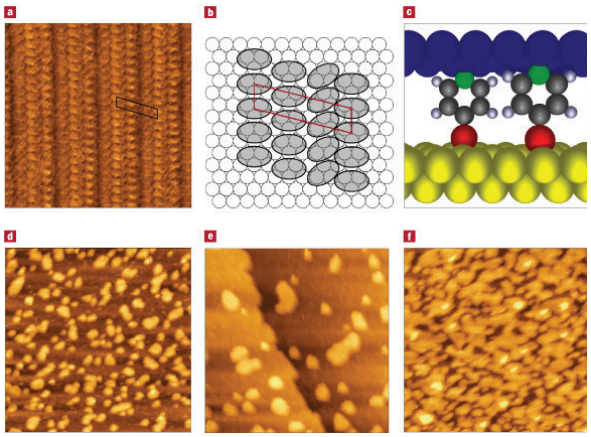

Mercaptopyridine double decker

F. Eberle, M. Saitner, H.-G. Boyen, J. Kucera, A. Groß, A. Romanyuk, P. Oelhafen, M. D'Olieslaeger, M. Manolova and D. M. Kolb, Angew. Chem. Int. Ed. **49**, 341 (2010).

Pt/Mpy/Pd/Mpy/Au(111) double decker

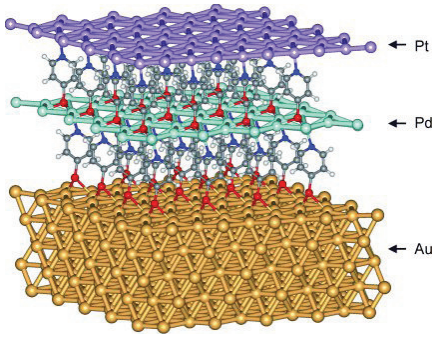

Model based on DFT structure optimization
Double-layer structure confirmed by angle-resolved XPS measurements

Water interaction with Pd/Mpy/Au(111) contact

Jan Kucera and Axel Groß, Beilstein J. Nanotech. **2**, 384 (2011).

H_2O monomer adsorption

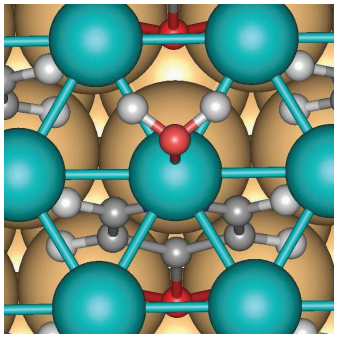

$\Theta_{H_2O} = 1/3$

$E_{ads} = -1.060\,eV$

Charge density difference

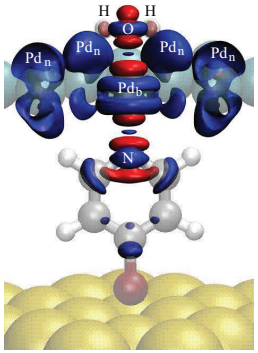

Strongly adsorbed water monomer due to polarization induced by the Pd-N bond

Water layer on Pd/Mpy/Au(111)

Jan Kucera and Axel Groß, Beilstein J. Nanotech. **2**, 384 (2011).

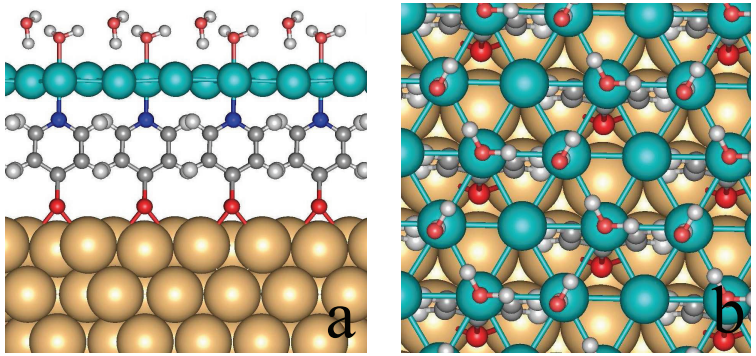

$\Theta_{H_2O} = 2/3,$ $E_{ads} = -0.837\,eV$

Tightly bound water layer due to strong water monomer adsorption

Hydrogen layer on Pd/Mpy/Au(111)

Jan Kucera and Axel Groß, subm. to PCCP

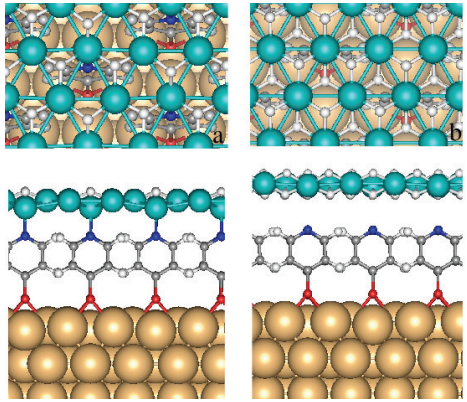

In an aqueous environment under standard conditions, Pd layers will always be hydrogen-covered

Conclusions

The theoretical description of processes on surfaces based on first-principles electronic structure calculations is able to elucidate microscopic mechanisms and thus contributes to enhance our understanding of electrochemical processes at the solid-liquid interface

Acknowledgments

Uni Ulm

Chong Gao
Yoshi Gohda
Jan Kucera
Daniela Künzel
Xiaohang Lin
Thomas Markert
, 165, 129.)Christian Mosch
Tanglaw Roman
Sebastian Schnur
Katrin Tonigold
TU München

Ataollah Roudgar
(now Vancouver, Canada)

Funding

DFG (German Science Foundation)
DAAD (German Academic Exchange Servive)
AvH (Alexander-von-Humboldt Foundation)
Baden-Württemberg Stiftung
Adenauer Stiftung

Computer time

NIC (John-von-Neumann Computing Center, Jülich)
kiz (Computer Center, Ulm University)
bwGrid